Journal of Thermal Analysis, Vol. 48 (1997) 349-358

THERMALLY STIMULATED DEPOLARIZATION CURRENT OF NOVOLAC RESIN
Influence of water and molecular weight on β relaxations

*M. Topić and Z. Katović**

Laboratory for Solid-State Chemistry, Ruder Bošković Institute, POB 1016, Zagreb, Croatia
*Chromos, Chemical Research Centre, 41000 Zagreb, Croatia

Abstract

A novolac phenol-formaldehyde resin was investigated via the thermally stimulated depolarization current, using integral and partial measurements in the temperature range from 137 to 270 K. Tow broadened peaks, assigned as β_1 and β_2, appeared at about 160 and 190 K. The influence of water and $\overline{M}_n$ was investigated. The activation energy E_a *vs.* T relationship was analysed, and a search was made for compensation phenomena. The distribution of the relaxing dipoles N *vs.* E_a was approximated. Three different relaxation ranges were distinguished. All the motions were attributed to the rotation of the phenyl rings. The differences found are due to the heterogeneity in the resin. Contamination with water increases the polarizability, decreases the structure differences and relieves the motions in the resin. A resin with a smaller $\overline{M}_n$ exhibits a higher polarizability and a decreases in structure variety.

Keywords: novolac resin, thermally stimulated depolarization current

Introduction

Characterizations of a novolac phenol-formaldehyde (NPF) resin by measurements of thermally stimulated depolarization current (TSDC) were performed in 1978 and 1980 [1, 2]. The dipolar α relaxation at 320 K and the space charge ρ relaxation at 334 K were described in 1984 [3]. The investigation of NPF by TSDC in a lower temperature range has recently been described [4]. The integral measurements revealed two broadened peaks, β_1 and β_2, with maximum current at 158 and 187 K, respectively. Application of the partial polarization technique [5] in the range from 145 to 210 K and analysis of the relaxation map [6] made it possible to distinguish three groups of processes. Only one group was considered to be a free relaxation with the compensation point T_c close to the related T_g. The other groups displayed irrational T_c's and a very narrow width in activation energy, ΔE_a, due to the inhibited motions. All the processes were presumed to be related to the motions of the phenyl rings around methylene links. The investigation was performed on a resin with $\overline{M}_n = 603$. The samples were prepared, stored and measured under relatively dry conditions. It was therefore of interest to study the influence of water on the properties of the resin.

0368–4466/97/ $ 5.00

John Wiley & Sons Limited
Chichester

Hydrogen-bonding in NPF, with and without water molecules, plays a significant role in forming the structure of novolacs [7]. The resin itself, without water, forms non-planar and coiled chains of novolac molecules due to the hydrogen-bonding. The strength of the hydrogen-bonding increases with the interpolation of water. After being dried at temperatures around 150°C, novolac resin still contains an appreciable amount of water, even up to 2%. On the other hand, novolac resin in the powder form left in 100% relative humidity at room temperature readily absorbs water, with transformation into a viscous liquid phase [8].

The aim of this work was to perform TSDC measurements in the β range, on NPF resin samples with different values of $\overline{M}_n$ and different contents of water.

Experimental

Novolac resin was prepared according to the general procedure [9]. The reactants were analytical grade, with a phenol to formaldehyde mole ratio of 1:0.80, and 1% oxalic acid based on the phenol charge. Reaction was carried out at the boiling temperature for 2 h, during which 98% of the formaldehyde was consumed. The water was decanted off and the unreacted phenol was removed by steam distillation. The resin was dehydrated by heating up to 170°C. The average molecular weight, $\overline{M}_n$, determined by GPC for sample B, was 603. Low molecular novolac, sample A, was obtained from novolac B by extraction with chloroform. It contained predominantly dimer and trimer oligomers, with $\overline{M}_n$=290. The remaining resin, sample C, was purified from chloroform traces by steam distillation, and had $\overline{M}_n$= 681. GPC was carried out as described elsewhere [10, 4]. The related curves are shown in Fig. 1. The resin samples were kept relatively dry in a desiccator over P_2O_5, unless otherwise stated. The resin was melted between two silver-coated brass electrodes with a diameter of 13.6 mm at a distance of 1 mm. The TSDC measurements were carried out in a dark cell filled with dry nitrogen. The polarization was performed with an electric field E_p=20 kV cm^{-1} at temperature T_p for 20 min. Partial polarization was performed with E_p=10 kV cm^{-1} for 10 min at different T_p, cooling to (T_p–5) K under E_p for about 5 min and cooling to the storage temperature T_0 (127 K) in the short-circuit state. The heating rate was 2 °C min^{-1}. Other details may be found elsewhere [4].

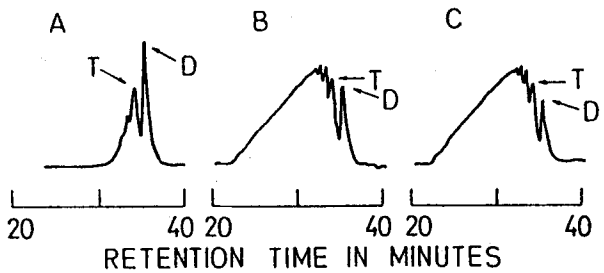

Fig. 1 GPC curves of NPF resin with different $\overline{M}_n$: (A) 290, (B) 603, (C) 681. Peaks: (D) dimer, (T) trimer

Results and discussion

Integral TSDC measurements

Integral TSDC measurements, sometimes called total or global, are runs with prolonged polarization over the entire temperature range from T_p to T_0. Such experiments were carried out on NPF samples with different $\overline{M}_n$ in the range from 137 to 270 K. Curves with two broadened peaks, β_1 and β_2, are shown in Fig. 2. The small and non-reproducible peaks at the end of the curves are caused by the discharge of teflon spacers in the sample cell. Curve B is related to the primary batch of resin, curve A to the low molecular fraction, and curve C to the high molecular residue. In order to consider the net depolarization current , the parasitic zero current had to be approximated and subtracted from the total current (dashed lines in Fig. 2). The approximation was performed by use of the runs with the polarized empty cell [4]. It can be seen that curves B and C practically do not differ, while for the low molecular resin the maxima of the peaks are increased and the distance between them is decreased. Such an increase in the peaks for a system with lower $\overline{M}_n$ was also observed for fluorinated NPF resin [11]. Obviously, the polarization field is more efficient when applied to the material with lower $\overline{M}_n$, causing an increase in polarization and a consecutive depolarization effect.

As concerns the influence of water on the NPF resin, three different TSDC curves are presented in Fig. 3. Curve B is the same as in Fig. 2. The resin powder was kept over P_2O_5 before melting. The run was performed under relatively dry conditions. Curve B′ was obtained with the same resin, but the sample cell was filled with air of about 60% relative humidity at room temperature. For curve B″, the resin, as the powder before melting, was kept under 100% relative humidity for

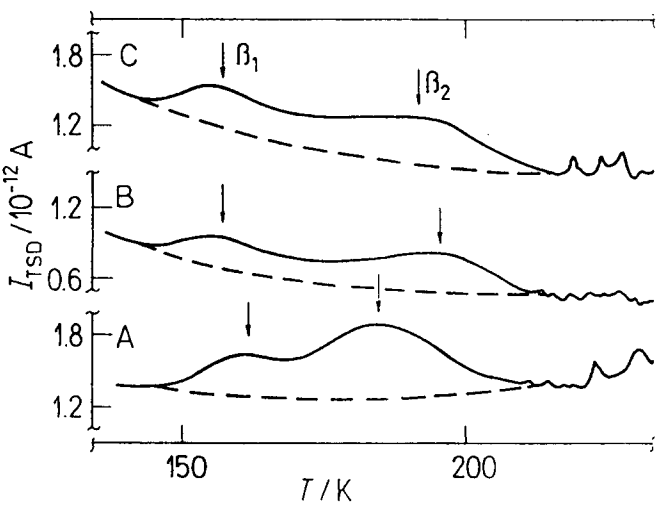

Fig. 2 Thermally stimulated depolarization current I_{TSD} *vs.T* for samples with different $\overline{M}_n$: (A) 290, (B) 603, (C) 681. E_p=20 kV cm^{-1}, T_p (for A)=285 K, (for B and C)=303 K. Vertical arrows show the maxima in the β_1 and β_2 peaks

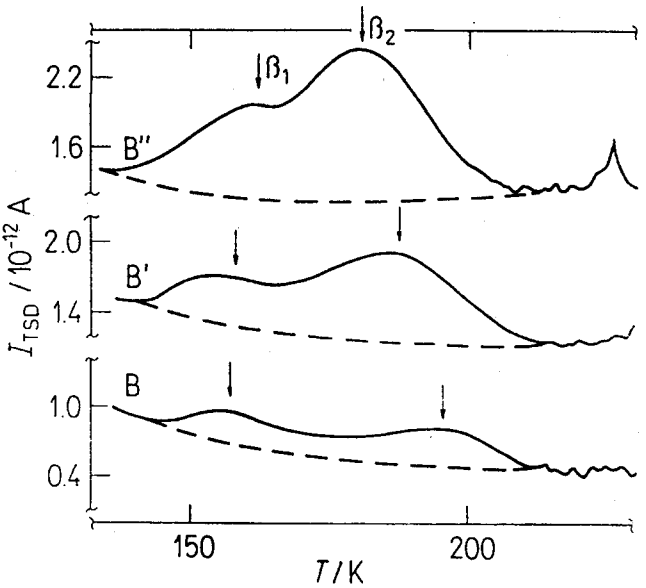

Fig. 3 $I_{TSD}(T)$ curves of samples with different contents of water: (B) relatively dry, (B′) exposed to 60% relative humidity at 298 K, (B″) exposed to 100% humidity. E_p=20 kV/cm, T_p=303 K

12 h, and the measurement was performed in the cell with air as was the case for B′. Comparison of the curves reveals that the water significantly influenced the TSDC, which increases with increase of the water content. The other effect is the shift of the maxima in the peaks, as for the low molecular resin. This effect seems to be related to the decrease in differences in the resin structure.

Partial polarization

A better way to characterize the relaxation processes is to apply the partial polarization technique. The polarization field is applied within a narrow temperature window, followed by a short-circuit to isolate a narrow relaxation part [5]. Results for samples with different amounts of water are given in Fig. 4. Each point represents the maximum net current I_m, and the corresponding temperature T_m, of the elementary peaks obtained by partial polarization. The results for resin sample B were published earlier [4]. Comparison of the results for B, B′ and B″ shows that the maximum peaks in the β_2 region (dashed arrows) significantly increase with increase of the water content and shift towards lower temperatures. A similar influence of water was observed for solid amylose. The effect was attributed to the plasticizing action of the loosely bond water. The peak disappeared after dehydration [12]. However, this does not mean that the peak is caused by water molecules themselves: the hydrogen-bonded water molecules increase the dipole moments of the

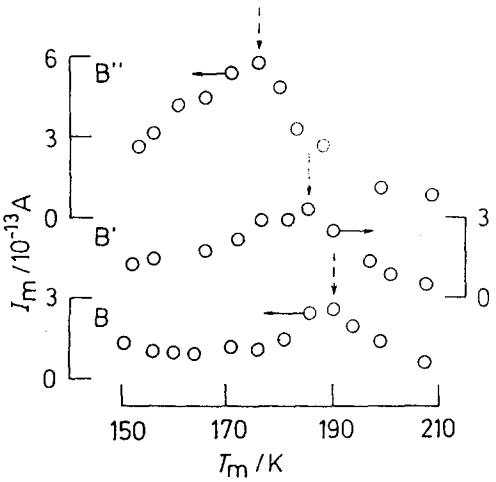

Fig. 4 Parameters of elementary peaks obtained by partial polarization for samples with different contents of water. Dashed arrows relate to the maximum amplitude peaks in the β_2 range. Symbols of samples as in Fig. 3

moving parts in the resin. In such a way, the water acts as a marker, which makes the motions in the resin more easily observable.

Figure 5 contains results on the activation energies of the elementary peaks for samples B, B′ and B″. E_a was determined by the Christodoulides method [13] by use of the equation:

$$E_a = \frac{T_1 T_m}{7940(T_m - T_1)} - \frac{T_1}{14866}$$

where T_1 is the temperature relating to $I_m/2$ (low-temperature side) and T_m is the temperature of the peak maximum. It is considered that the Christodoulides method is more accurate and more practical, especially for the small peaks, than the well-known initial rise method. All the results for E_a were divided into three distinctive groups and presented by the most probable lines l_1, l_2 and l_3. The first group relates to the β_1 region, the second group to the initial part of β_2 and the third group to the final part of β_2. The dashed arrows show the points relating to the maximum peaks. For further analysis and calculations, the elementary values E_a will be corrected to fit the lines l_1, l_2 and l_3. E_a in the β_1 range for resin B, as already described [4], increases slightly with temperature. The difference between the maximum and the minimum E_a, ΔE_a, was very narrow and equal to 0.013 eV. The mean energy $\overline{E}_a$ for β_1 was 0.52 eV.

The change of E_a *vs.* T in the β_1 range for other samples is difficult to discuss, because of the small number and high dispersion of the points. However, it can be stated that ΔE_a for β_1 is generally very narrow. E_a in the starting and the final parts of β_2 increases with temperature for all samples, but the slopes for l_3 are more or

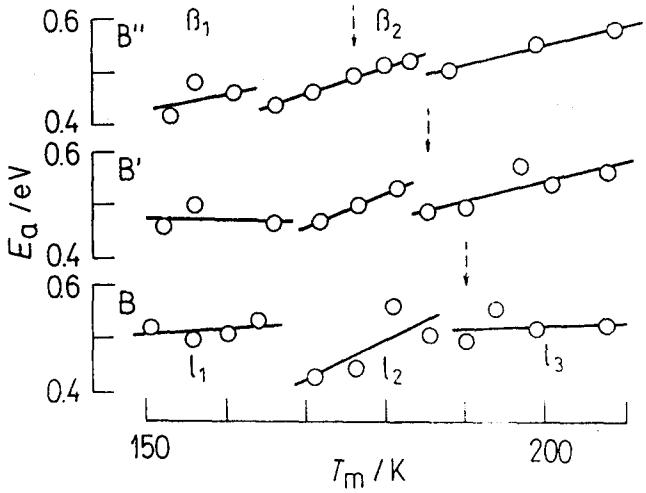

Fig. 5 E_a *vs.* T_m for elementary peaks relating to Fig. 4: fitting lines l_1, l_2 and l_3

less reduced in comparison with those for l_2. The presence of water decreases the difference between the slopes. A comparison of $\overline{E}_a$ and ΔE_a for all ranges and samples is given in Table 1. The data are based on the corrected E_a's against the fitting lines. It can be seen that the differences between the $\overline{E}_a$ values for β_1 and β_2 are in all cases less than 0.1 eV. This supports the proposition that both peaks are caused by the same motions, e.g. the rotation of the phenyl rings around methylene links [4].

Table 1 Mean activation energy

Range		B		B'		B''	
		$\overline{E}_a$	ΔE_a	$\overline{E}_a$	ΔE_a	$\overline{E}_a$	ΔE_a
		eV					
β_1	l_1	0.515	0.013	0.473	0.004	0.449	0.025
β_2	l_2	0.485	0.107	0.502	0.064	0.487	0.087
	l_3	0.523	0.012	0.531	0.084	0.548	0.076

Compensation phenomena

In order to study the compensation phenomena, it is necessary to determine the Arrhenius line for each of the elementary peaks according to the equation:

$$\ln\tau = \ln\tau_0 + E_a/kT$$

where τ is the relaxation time, τ_0 is the pre-exponential factor and k is the Boltzmann constant. The collection of Arrhenius lines called the relaxation map shows the relation between the relaxation behaviour of the elementary peaks. The

compensation phenomenon is the case when the lines converge to a point called the compensation point at the compensation temperature T_c and compensation time τ_c. The existence of several compensation points is due to the separate ordering of motion in the amorphous state [14]. Instead of drawing the relaxation map, the compensation, if any, can be determined by the compensation line [15]:

$$\ln\tau_o = -E_a \times 1/kT_c + \ln\tau_c$$

The drawn line gives all the data about the compensation. $\ln\tau_c$ is the intercept, while the negative slope is $1/kT_c$. The abscissa projection shows ΔE_a for the related relaxation. In a system with more than one compensation point, the distance between the compensation lines indicates the differences between the regions, domains or phases [14].

Compensation lines for resin containing different amounts of water are shown in Fig. 6. All data are derived from the elementary peaks obtained by partial runs. Lines d_2 relate to the initial parts of β_2, and d_3 to the final parts of β_2. Analogous results for the β_1 region are omitted due to the uncertainty in E_a. $\ln\tau_o$ for an elementary peak is calculated according to:

$$\ln\tau_o = \ln\tau(T_m) - E_a/kT_m$$

and

$$\tau(T_m) = Q(T_m)/I_m$$

where $\tau(T_m)$, $Q(T_m)$ and I_m are the relaxation time, residual charge and current at the temperature of the elementary peak maximum. For E_a, the corrected data fitting lines l_2 and l_3 are used. The calculated compensation parameters are listed in Table 2. The split in the β_2 peaks in the two ranges d_2 and d_3 is due to the heteroge-

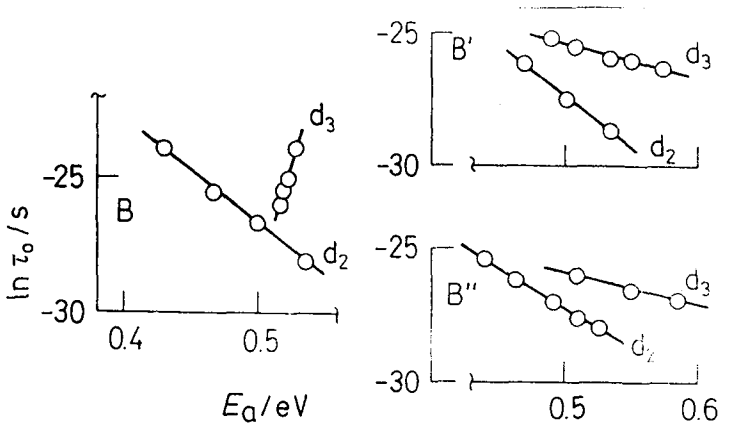

Fig. 6 Compensation diagram $\ln\tau_o$ *vs.* E_a for samples with different contents of water: d_2 relates to initial part of β_2, d_3 relates to final part of β_2. Symbols of samples as in Fig. 3

Table 2 Compensation parameters for resin with different amount of water

Range	B		B′		B″	
	T_c/K	τ_c/s	T_c/K	τ_c/s	T_c/K	τ_c/s
d_2	308	4.25×10^{-4}	298	3.68×10^{-4}	388	4.9×10^{-6}
d_3	−67[a]	5.1×10^{-51}	908	5.7×10^{-9}	975	2.2×10^{-9}

[a] Irrational result

neity in the resin, which causes differences in the relaxation parameters. The most characteristic compensation for the resin is that presented by lines d_2. T_c for B is only 26°C below T_g obtained by DSC, which is a good coincidence. T_c for B′ and B″ show a shift, but not more than 80 deg for B″, which means that the influence of water is very moderate. However, in the range covered by compensation lines d_3, the influence of water is significant. T_c is shifted from the irrational −67 K for B to 908 and 975 K for B′ and B″, respectively. Since an irrational T_c is an indication of a rigid structure and processes with extremely low ΔE_a, it can be presumed that the transition from irrational to rational T_c is due to the changes in structure, which becomes more flexible. A comparison of all the lines in Fig. 6 shows that the differences in their positions decrease with the increase of the water content. In conclusion, water decreases rigidness as a lubricant, making the structure more flexible and uniform.

Distribution of activation energy

An important method for the characterization of polymeric systems is determination of the energy distribution function $N(E_a)$ [16], where N is the relative number of dipoles in a sample which take part in the relaxation. A simplified method for approximation of the energy distribution by use of the three extreme values has recently been proposed [17]. Figure 7 contains the ln $N(E_a)$ approximations for the entire β_2 range for samples B, B′ and B″. N was approximated by use of the equation [16]:

$$N = I_m \times T_m$$

For determination of the points, the elementary peaks were used. I_m, T_m and E_a values are shown in Figs 4 and 5. The E_a's are corrected to fit the lines l_2 and l_3. E_a(I) and N(I) are related to the minimum energy peaks in the β_2 range. E_a(II) and N(II) relate to the peaks with maximum amplitude (dashed arrows), and E_a(III) and N(III) to the maximum energy peaks. All the values of ln$N$ were normalized to ln$N$(II) = 10 for B″. The distributions were characterized by widths ω at heights equal to 80% of the maximum value (Table 3). It can be seen that the presence of water in B″ increases ω significantly. As already shown [17], the increase in ω is a consequence of an increase in flexibility of the consitituents in the polymeric system. It is therefore evident from another point of view that the presence of water relieves the motions in the resin.

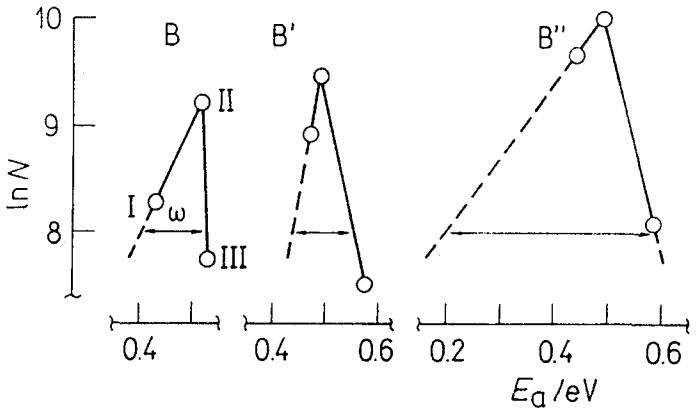

Fig. 7 Activation energy distribution in β_2 range for samples with different contents of water; (N) approximate number of dipoles, (ω) distribution width at 80% of maximum value, (I), (II) and (III) extreme values, according to Table 3. Symbols of samples as in Fig. 3

Table 1 Parameters for distribution of the activation energy for β_2 range. Related to elementary peaks. (I) Determined from minimum energy peaks; (II) determined from maximum amplitude peaks; (III) determined from maximum energy peaks

Samples	ln$N$			E_a/eV			ω/eV
	(I)	(II)	(III)	(I)	(II)	(III)	
B	8.28	9.22	7.73	0.43	0.52	0.53	0.12
B'	8.93	9.46	7.51	0.47	0.49	0.57	0.12
B''	9.67	10.00	8.09	0.44	0.49	0.59	0.41

Conclusions

The analysis of NPF resin by integral and partial measurements in the β temperature range form 137 to 270 K shows two current peaks, β_1 and β_2, with maxima at about 160 and 190 K, respectively. The samples with low $\overline{M}_n$ demonstrate an increase in the amplitude of the peaks due to the increase in polarizability. The maxima in β_1 and β_2 shift relative to each other. It is proposed that this is caused by the decrease in structure differences.

The presence of water increases the dipole moments of the moving parts and therefore increases the polarizability of the resin. The maxima in the peaks are shifted similarly as in the system with low $\overline{M}_n$. Analysis of the results for $E_a(T)$ and ln $\tau_0(E_a)$, based on the partial measurements, allows the distinction of three different relaxation ranges, caused by heterogeneity in the resin. The first range, relating to β_1, exhibits a narrow ΔE_a due to the inhibited motions. The second range, relating to the starting part of β_2, represents the relaxations with T_c not very far from T_g,

with a moderate influence of water. The third range, relating to the final part of β_2, represents the relaxations very sensitive to the water content, which relieve motions and decrease the heterogeneity. The $\overline{E}_a$ values for all the ranges for resin containing different amounts of water do not differ by more than 0.1 eV. It is proposed that all the relaxations are caused by the unique motion of the phenyl rings around the methylene links with different surrounding structures. The characterization of samples by the approximate distribution $N(E_a)$ shows that water increases the distribution width ω essentially, due to the increase in flexibility of the resin.

* * *

The authors are grateful to Professor S. Popović for helpful discussion and for a critical reading of the manuscript.

References

1 M. Goel, P. S. Viswanathan and P. Vasudevan, Polymer, 19 (1978) 905.
2 P. Vasudevan, P. S. Viswanathan and K. L. Taneja, J. Electrochem. Soc., 127 (1980) 691.
3 M. Topić, A. Moguš-Milanković and Z. Katović, Phys. Status Solidi, A 86 (1984) 413.
4 M. Topić and Z. Katović, Polymer, 35 (1994) 5536.
5 C. Lacabanne, D. Chatain, J. Guillet, G. Seytre and J. F. May, J. Polym. Sci. Polym. Phys. Ed., 13 (1975) 445.
6 A. Bernes, R. F. Boyer, D. Chatain, C. Lacabanne and J. P. Ibar, in Order in the Amorphous State of Polymers. S. E. Keinath, R. L. Miller, J. K. Rieke (Eds), Plenum Publishing, New York 1987, p. 305–326.
7 M. F. Drumm and J. R. Le Blanc, The Reactions of Formaldehyde with Phenols, Melamine, Aniline and Urea, in Kinetics and Mechanism of Polymerization, G. E. Ham, D. H. Solomon (Eds), Marcel Dekker, Inc., New York 1972, Vol. 3, p. 204–214.
8 Z. Katović, Some Aspects of the Curing Processes in Phenolic Resins, in Weyerhaeuser Science Symposium, Phenolic Resins, Chemistry and Application, Weyerhaeuser Company Tacoma, Washington 1981, p. 85–103.
9 A. Knop, V. Böhmer and L. A. Pilato, Phenol-Formaldehyde Polymers, in Comprehensive Polymer Science, Pergamon Press., Oxford 1988, Vol. 5, p. 630–633.
10 M. Topić, A. Moguš-Milanković and Z. Katović, Polymer, 32 (1991) 2892.
11 M. Topić and Z. Katović, Angew. Makromol. Chem., 178 (1990) 33.
12 K. Nishinari, D. Chatain and C. Lacabanne, J. Macromol. Sci. Phys., B22 (1983) 529.
13 C. Christodoulides, J. Phys. D: Appl. Phys., 18 (1985) 1501.
14 A. Saadat, A. Bernes, P. Cebeillac, A. Lamure, D. Chatain and C. Lacabanne, IEEE Trans. Electr. Insul., 25 (1990) 630.
15 C. Lacabanne and D. Chatain, in Charge Storage, Charge Transport and Electrostatics with their Applications, Y. Wada, M. M. Perlman, H. Kokado (Eds), Elsevier, Amsterdam 1979, p. 312–316.
16 A. L. Kovarskii, S. A. Mansimov and A. L. Buchachenko, Polymer, 27 (1986) 1014.
17 M. Topić and Z. Veksli, Polymer, 34 (1993) 2118.